RSC Advances

ROYAL SOCIETY OF CHEMISTRY

www.rsc.org/advances

Cite this: DOI: 10.1039/c0xx00000x

www.rsc.org/xxxxxx

ARTICLE TYPE

Synthesis and infrared shielding property of molybdenum-containing ammonium tungsten bronze

Tingyu Wang[a], Yan Li[a], Junping Li[b], Zhihai Feng[b], Dongfeng Sun[a], Bin Zhao[a], Yaohui Xu[a], Ruixing Li[a,*], Hongnian Cai[c,*]

Received (in XXX, XXX) Xth XXXXXXXXX 20XX, Accepted Xth XXXXXXXXX 20XX
DOI: 10.1039/b000000x

A series of molybdenum-containing ammonium tungsten bronze was synthesized by a solvothermal process at 200 °C for 72 h using ethylene glycol, acetic acid, ammonium tungstate and ammonium molybdate as starting materials. All the diffraction peaks of XRD for the samples synthesized with starting Mo/W (mol.) = 0 − 0.2 could be rough indexed as a hexagonal ammonium tungsten bronze with the formula of $(NH_4)_{0.33}WO_3$, which accompanied with a shift of main peaks after introduction of molybdenum and a split peak for starting Mo/W (mol.) = 0.1. Content of nitrogen, based on both the thermogravimetry and X-ray photoelectron spectroscopy, rose with the increase of molybdenum content. Optical property was evaluated using the Fourier transform infrared spectrometer, which proved that the molybdenum-containing ammonium tungsten bronze could shield infrared rays better than the sample without molybdenum. And the shield efficiency was related with the content of molybdenum. The optimum starting Mo/W (mol.) to obtain high infrared shielding property was 0.1. This sample consisted of uniform rods of *ca*. 50 nm in diameter emerging from the agglomerates.

1. Introduction

Tungsten bronzes are a group of nonstoichiometric compounds with the general formula M_xWO_3. In the most cases, structure of tungsten bronzes is built up of layers containing corner-sharing WO_6 octahedra. The edges of WO_6 octahedra form triangular, quadrangular, pentagonal or hexagonal channels, which are occupied randomly by cations.[1]

It had been deeply researched due to the interesting physical and chemical properties, such as electronic and magnetic properties, superconductivity, gas sensors, ionic conductivity.[2, 3] In recent years, nanoparticles of hexagonal tungsten bronzes attract more and more attention because of the excellent near-infrared (NIR) shielding property. Guo et al.[4–8] synthesized various nanoparticles of tungsten bronzes with different cations in the channels, such as Na^+, K^+, Rb^+, Cs^+, or NH_4^+, by facile hydrothermal or solvothermal approach, and investigated their near-infrared shielding property. Comparing with the conventional near-infrared shielding materials, such as nanoparticles of rare-earth hexaborides and tin-doped indium oxide (ITO),[9–11] tungsten bronzes have better performance of NIR shielding and visible light transmitting, and can be prepared with relatively facile routes.

Adachi and Sato[12–14] researched and discussed the origin of the NIR absorption of tungsten bronzes which is caused by a localized surface plasmon resonance. This phenomenon is observable for the one-dimensional nanoparticles because transverse and longitudinal surface plasmon resonances correspond to electron oscillations perpendicular and parallel to the length direction, respectively.[6,8] Moreover, amount of free electrons also affect the NIR shielding property.[15] In the channels of hexagonal tungsten bronzes, each cation contributes one electron to the tungsten conduction band.[16] Consequently, the amount of cations, *i.e.*, the value of x in M_xWO_3 influence the NIR shielding property. In addition, the optical property of nanosized particles also relate to the crystallographic defects.[17, 18] On the basis of these theories, it is possible to improve the NIR shielding property by doping of tungsten bronzes.

From the viewpoint of crystal chemistry, most of the reported researches about infrared shielding property of tungsten bronzes focused on different cations in the channels. These tungsten bronzes have almost identical crystalline structures and similar chemical composition, *i.e.*, a series of isomorphism. There were few works about doping onto the tungsten site and the effect on the infrared shielding property. In the present paper, molybdenum-containing ammonium tungsten bronze was synthesized by a solvothermal process. At a certain molybdenum concentration, molybdenum-containing ammonium tungsten bronze formed clear rod-like morphology and possessed homogeneous diameter. This sample had lower infrared transmittance than that of the ammonium tungsten bronze without molybdenum.

2. Experimental

0.5 g ammonium tungstate and a certain amount of ammonium molybdate were dissolved into 20 ml ethylene glycol at 190 °C. After cooling down this ethylene glycol solution to the room temperature, 10 ml acetic acid was added into the solution. Then, the obtained solution was transferred into an autoclave of 50 ml internal volume, followed by solvothermal reaction in an electric oven at 200 °C for 72 h. After the reaction, the powder was centrifuged, washed 4 times with water and ethanol, respectively, and finally dried.

The phase compositions of the samples were determined by X-ray diffraction analysis (XRD, Rigaku D/max 2200 PC) using graphite monochromatized Cu Kα radiation. The morphology and microstructure of the nanoparticles were investigated using scanning electron microscopy (SEM, Hitachi S-4800). The thermal behavior of the samples was investigated by the thermogravimetry and differential scanning calorimetry (TG-

DSC, Netzsch STA449F3) from room temperature to 700 °C at a heating rate of 5 °C·min^{-1} in air. The surface composition and binding energy of the samples were determined by X-ray photoelectron spectroscopy (XPS, ESCALAB 250). Concentrations of elements were determined using inductively coupled plasma-atomic emission spectrometer (ICP-AES, SPECTRO ARCOS EOP).

To investigate the optical performance of molybdenum-containing $(NH_4)_xWO_3$ powder, an infrared measurement was employed by a Fourier transform infrared spectrometer (FT-IR, Tensor 27). The method is to grind a known mass ratio (100 : 1) of potassium bromide and the as-synthesized sample, and then pressed in a mechanical press with a constant pressure to form a pellet to ensure the results under the same condition.

3. Results and discussion

XRD analysis was employed to identify the phase composition and crystallographic structure of the samples. Figure 1 shows the XRD patterns of the samples prepared with various Mo/W (mol.) in the starting materials and the product synthesized by ammonium molybdate without ammonium tungstate under the same reaction conditions. Figure 1(a) shows the XRD pattern of $(NH_4)_xWO_3$ without molybdenum. All the diffraction peaks of this sample could be well indexed as the hexagonal ammonium tungsten bronze with the formula $(NH_4)_{0.33}WO_3$ (JCPDS card no.42-0452), and no characteristic peaks for impurities are observed. Higher diffraction intensity for the sample synthesized with starting Mo/W (mol.) of 0.05 can be seen in Fig. 1(b). Figure 1(c) shows the sample prepared with starting Mo/W (mol.) of 0.1. To understand XRD results more clearly, magnification patterns can offer easy viewing minor response for the introduction of molybdenum, as shown in Fig. 2. It is worth noting that the (002) diffraction peak of the product with Mo/W (mol.) = 0.1 splits into two peaks as shown in Fig. 2(b). It implies an existence of some species for this sample, although they are not able to be identified. Moreover, an obvious shift for both (002) and (200) diffraction peaks of the sample towards larger degree can be found comparing to the sample without molybdenum, as shown in Fig. 2(a). It may be attributed to the doping. Figures 1(d) and (e) show the samples synthesized with starting Mo/W molar ratios of 0.15 and 0.2, respectively. All the peaks are consistent with $(NH_4)_{0.33}WO_3$. A magnification result for the ratio of 0.20 as shown in Fig. 2(c), a slight shift only for (200) is exhibited. In addition, an amorphous phase was obtained according to the pattern of the sample synthesized from ammonium molybdate without ammonium tungstate, as shown in Fig. 1(f). It might be a kind of ammonium-containing molybdenum oxides. An in-depth discussion is to follow.

To clarify the effects of the introduction of Mo on the characteristics of $(NH_4)_xWO_3$, the morphologies of the samples were observed by SEM, as shown in Fig. 3. Figure 3(a) shows the sphere-like morphology of the product synthesized from ammonium molybdate without ammonium tungstate. These sphere-like particles should be the amorphous ammonium-containing molybdenum oxides combined with Fig. 1(f). Nonuniform rod-like particles can be observed for the samples synthesized with starting Mo/W (mol.) of 0 and 0.05, as shown in Figs. 3(b) and 3(c). Figure 3(d) displays uniform rods of *ca*. 50 nm in diameter emerging from the agglomerates for the sample synthesized with starting Mo/W (mol.) of 0.1 . Although there might be some unknown species combined with the results from XRD (*see* Fig. 2b), there is no obviously difference in the

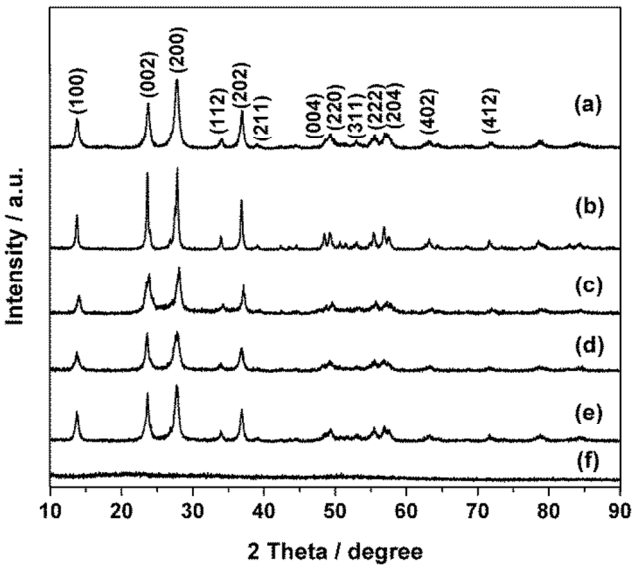

Fig. 1. XRD patterns of the samples with Mo/W (mol.) = (a) 0; (b) 0.05; (c) 0.1; (d) 0.15; (e) 0.2 in the starting materials; and (f) sample synthesized from ammonium molybdate without ammonium tungstate.

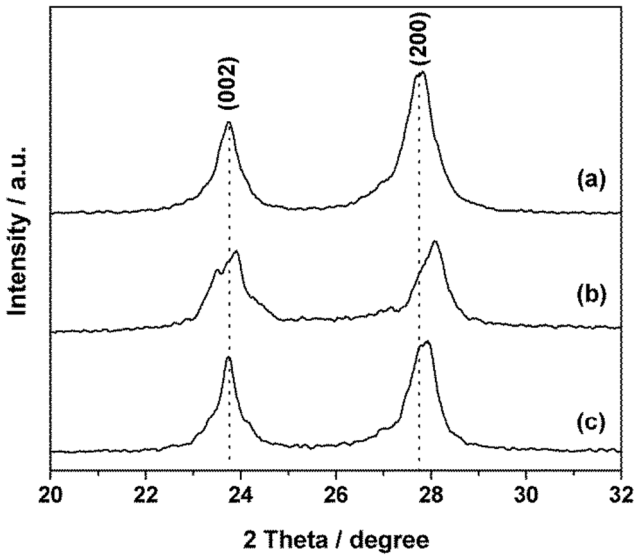

Fig. 2. XRD patterns of the samples with Mo/W (mol.) = (a) 0; (b) 0.1; (c) 0.2 in the starting materials.

morphology for this sample. When the starting Mo/W (mol.) is over 0.15, more and more sphere-like particles, which are similar to Fig. 3(a), can be found (*see* Figs. 3e and f). Obviously, right amount of Mo, *i.e.*, Mo/W (mol.) is 0.1, is beneficial to an evolution of uniform rod-like ammonium tungsten bronze. Related the morphologies (*see* Figs. 3a, e and f) with the results from XRD (*see* Figs. 1d, e, f and Fig. 2c), the amorphous ammonium-containing molybdenum oxides were slipped through for the XRD analysis, however, caught up in the electron microscopy observation. With the increase of Mo content in the starting materials, the excessive ammonium molybdate is adverse to fabricate doped sample and makes the internal stress in the lattice partly relax. Thus, the shift for the sample with Mo/W (mol.) = 0.2 is not strong enough than that of 0.1, as shown in Figs. 2 (b) and (c). Accompanying with a synchronous variation, it enables amorphous ammonium-containing molybdenum oxides

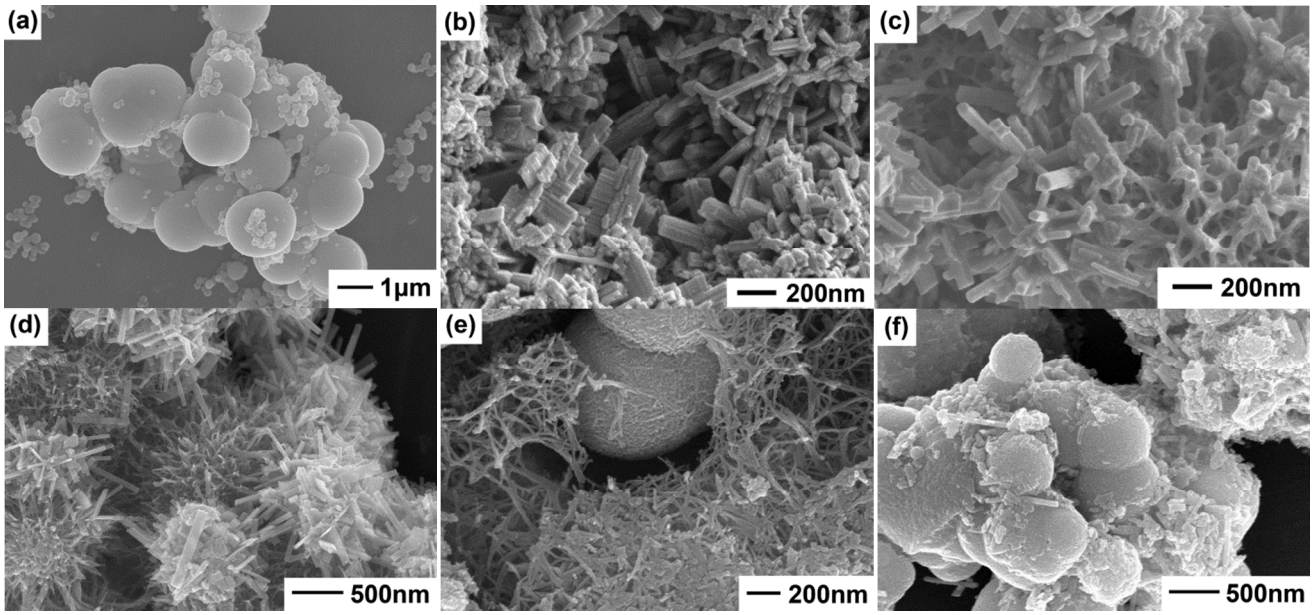

Fig. 3. SEM images of the samples (a) without tungsten; and with Mo/W (mol.) = (b) 0; (c) 0.05; (d) 0.1; (e) 0.15; and (f) 0.2 in the starting materials.

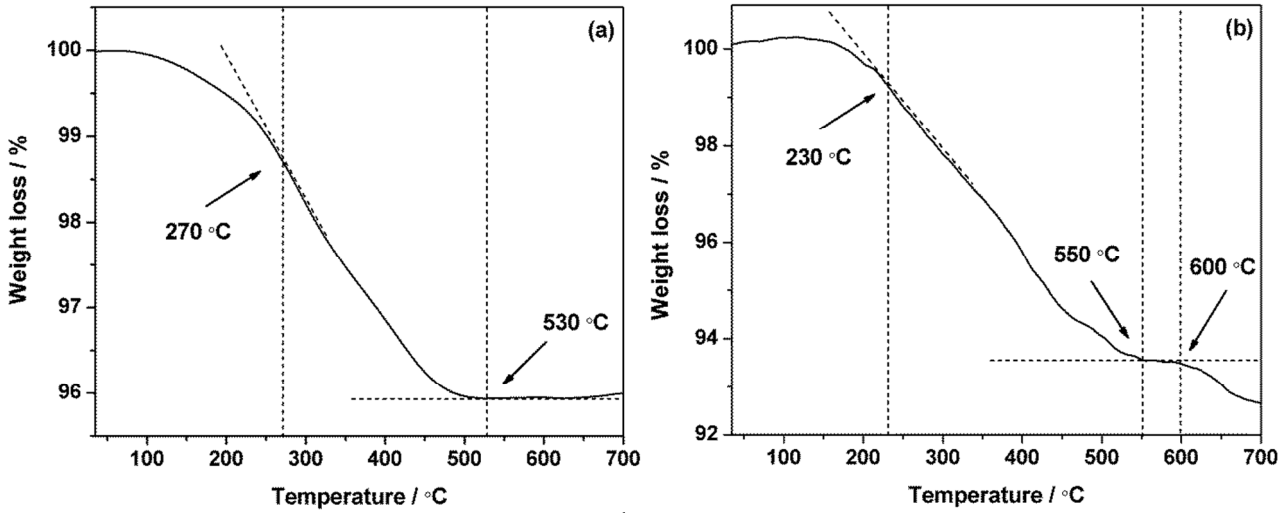

Fig. 4. TG curves recorded in air at a heating rate of 5°C·min^{-1} for the samples (a) without molybdenum and (b) with Mo/W (mol.) = 0.15 in the starting materials.

separate out from the solid solution of Mo-containing ammonium tungsten bronze, as shown in Figs. 3(e) and (f). Consequently, the above results suggest that the starting Mo/W (mol.) = 0.1 might be close to a saturation point for doping concentration, which leads to greater shift of diffraction peaks and maintains no sphere-like amorphous ammonium-containing molybdenum oxides.

The thermal behaviors of the samples synthesized with starting Mo/W (mol.) = 0 − 0.2 were further investigated. As shown in Fig. 4, the weight loss of $(NH_4)_xWO_3$ without molybdenum from room temperature to 100 °C could be related to the loss of surface adsorbed water. After that, the weight loss up to about 270 °C could be attributed to the loss of structural water. The weight loss in the temperature range of 270 − 530 °C can be explained as the release of NH_3 and H_2O because of the decomposition of $(NH_4)_xWO_3$. Previous researches had confirmed that the powder remained after 550 °C was WO_3.[8] Based on the weight of NH_3 decomposed from $(NH_4)_xWO_3$ and the weight of WO_3, the value of x (*i.e.*, molar ratio of N/W) in $(NH_4)_xWO_3$ without molybdenum could be calculated in terms of its thermogravimetric curve to be 0.26 which is lower than the theoretical maximum value of 0.33. Similar result of x was reported.[8] The trends of thermogravimetric curves for the products synthesized with starting Mo/W (mol.) of 0.05 and 0.1 are similar to Fig. 4(a). In the case of the sample with Mo/W (mol.) = 0.05, the value was calculated to be 0.32, which tracks more closely with the theoretical value of 0.33. Furthermore, this value is 0.46, over the theoretical value of 0.33 for the sample with Mo/W (mol.) = 0.1. However, there is an obvious difference after 600 °C for the thermogravimetric curves of samples with Mo/W (mol.) over 0.15, as shown in Fig. 4(b). It may be caused by the sublimation of molybdenum oxide based on the images of SEM and sublimation point of 600 °C for molybdenum oxide. The values of x for the samples synthesized with Mo/W (mol.) =

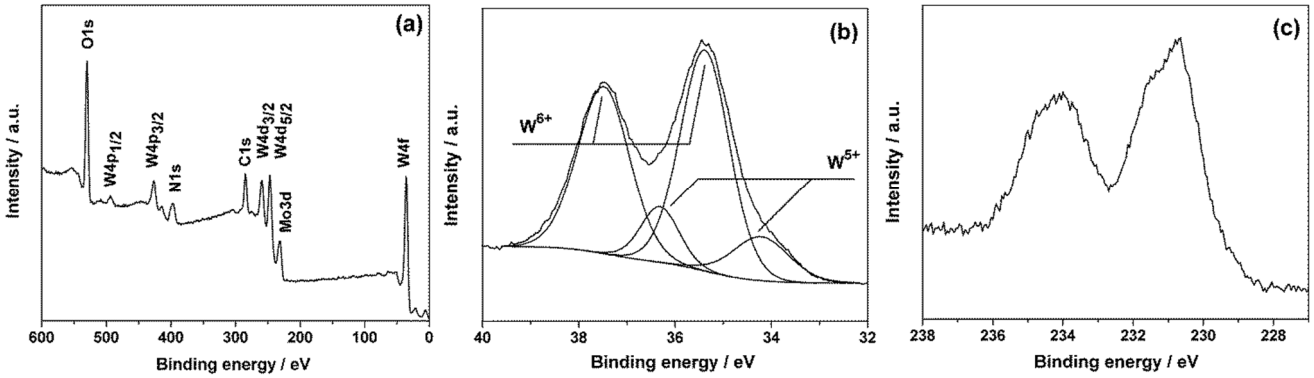

Fig. 5. XPS spectra of (a) full range; (b) W4f core-level; and (c) Mo3d core-level for Mo-containing $(NH_4)_xWO_3$ synthesized with starting Mo/W (mol.) = 0.1.

0.15 and 0.2 are 0.54 and 0.56, respectively. Clearly, the content of nitrogen rises with the increase of the Mo concentration in terms of its thermogravimetric curves. Combined with the split and shift of the diffraction peaks in XRD (*see* Fig. 2b), the unreasonable value of 0.46 for Mo/W (mol.) = 0.1 might be attributable to the molybdenum introduction. On the other hand, the values of 0.54 and 0.56 might be related to the amorphous ammonium-containing molybdenum oxides which are inclined to form molybdenum oxide during thermal decomposition.

The chemical composition and valence state for Mo-containing $(NH_4)_xWO_3$ were examined by XPS. Take the sample synthesized with starting Mo/W (mol.) = 0.1 for example, the fully scanned spectrum clearly shows that elements of N, W, Mo and C exist in the sample (Fig. 5a). The presence of carbon element in the final product may be related to the residual chemically or physically adsorbed organics originating from the solvent. The XPS peak of N1s may be related to the group of NH_4^+ in the ammonium tungsten bronze. For tungsten, a complex energy distribution of W4f photoelectrons was obtained as shown in Fig. 5(b). The W4f core-level spectrum could be well fitted into two spin-orbit doublets, corresponding to two different oxidation states of W atoms. And, the Mo3d photoelectrons were also detected, as shown in Fig. 5(c). The molar ratio of N/(W+Mo) on the surface is 0.43, which was determined by the atomic percentages of N, W and Mo. Additionally, the molar ratio of N/W of $(NH_4)_xWO_3$ without molybdenum is 0.24, which was determined likewise by XPS (elided). The above molar ratios, 0.24 and 0.43, are close to those calculated results of thermogravimetry. In a sense, this excessive nitrogen of 0.43 for the sample with Mo/W (mol.) = 0.1 further confirms the existence of some unknown N-containing species.

To determine the actual Mo concentration, both the sample and its mother liquid synthesized with starting Mo/W (mol.) of 0.1 were examined using ICP-AES. In this way, the actual molar ratio of Mo/W is 0.159 for the sample. This value is greater than 0.1 for the starting materials. Correspondingly, Mo/W (mol.) in the mother liquid is 0.016. Therefore, it could be calculated that the recovery ratios of W and Mo are about 59% and 94%, respectively. Thus, a higher recovery ratio of Mo leads to an increase in actual Mo/W molar ratio, which reaches 0.159 for the sample with starting Mo/W (mol.) = 0.1.

To investigate the infrared shielding property of Mo-containing $(NH_4)_xWO_3$, an infrared measurement was employed in a wide wavelength range. Figure 6 shows the transmittance of infrared for samples synthesized with Mo/W (mol.) in the starting materials between 0 and 0.2. Lower transmittance implies better infrared shielding property. Figure 6 exhibits that the sample

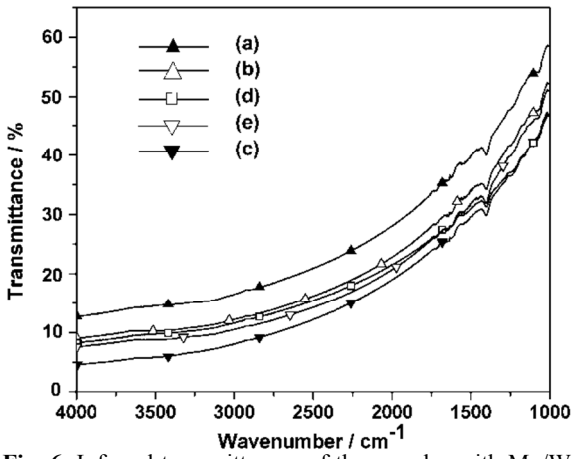

Fig. 6. Infrared transmittances of the samples with Mo/W (mol.) = (a) 0; (b) 0.05; (c) 0.1; (d) 0.15; and (e) 0.2 in the starting materials.

without molybdenum has the highest transmittance in the spectrum of wave number of 4000 − 1000 cm^{-1}. This result indicates that the infrared shielding property of Mo-containing $(NH_4)_xWO_3$ is superior to the product without molybdenum in this work. Transmittances of samples prepared with starting Mo/W (mol.) of 0.05, 0.15 and 0.2 (Figs. 6b, d and e) are closely adjacent to each other and lower than that of $(NH_4)_xWO_3$ without molybdenum in sequence. Specially, the sample synthesized with starting Mo/W (mol.) of 0.1 has the lowest transmittance, *i.e.*, the best infrared shielding property, as shown in Fig. 6(c). The lower transmittance of Mo-containing $(NH_4)_xWO_3$ may be attributable to the introduction of crystallographic defects deriving from molybdenum, which might be associated with higher content of nitrogen. For the sample with Mo/W (mol.) of 0.1, the molybdenum content might be close to the saturation point for the doping concentration, which contributes some more crystallographic defects. Thus more defects together with higher content of nitrogen achieve the best infrared shielding property. If the Mo/W (mol.) is over 0.15, excessive nitrogen tends to precipitate out the second phase of amorphous ammonium-containing molybdenum oxides. It had an effect on the infrared shielding property.

4. Conclusions

Mo-containing $(NH_4)_xWO_3$ was successfully synthesized by the

solvothermal process. The results of XRD confirmed that Mo was doped into $(NH_4)_xWO_3$. When the actual Mo/W (mol.) reached 0.159, *i.e.*, the starting Mo/W (mol.) of 0.1, the product was close to the saturated Mo doping concentration according to the results of XRD and SEM. And the value of x in $(NH_4)_xWO_3$ for this sample of Mo/W (mol.) = 0.1 achieved 0.46 in terms of its thermogravimetric curve or 0.43 on the basis of XPS, was higher than the theoretical maximum of 0.33. Its morphology was assembled from more uniform rod-like particles in diameter of *ca.* 50 nm. Moreover, this sample exhibited the lowest infrared transmittance in a wide wavelength range comparing to all the samples with or without molybdenum.

Acknowledgments

The authors appreciate the financial support from the National Science Foundation of China (NSFC51372006); the Scientific Research Starting Foundation for Returned Overseas Chinese Scholars, Ministry of Education; the Start-Up Fund for High-End Returned Overseas Talents (Renshetinghan 2010, No. 411), Ministry of Human Resources and Social Security, China and the Lab-Installation Foundation of Beihang University for New Teachers.

Notes and references

[a]*Key Laboratory of Aerospace Materials and Performance (Ministry of Education), School of Materials Science and Engineering, Beihang University, Beijing 100191, China*
E-mail: ruixingli@yahoo.com

[b]*Aerospace Research Institute of Materials & Processing Technology, No. 1 Nan Da Hong Men Road, Fengtai District, Beijing 100076, China*

[c]*China South Industries Group Corporation, No. 10 CheDaoGou Street, Beijing100089, China*
E-mail: caihn@cae.cn

1. I. M. Szilágyi, J. Madarász, G. Pokol, F. Hange, G. Szalontai, Katalin Varga-Josepovits and A. L. Tóth, *J. Therm. Anal. Calorim.*, 2009, **97**, 11.
2. S. Raj, T. Sato, S. Souma and T. Takahashi, *Mod. Phys. Lett. B*, 2009, **23**, 2819.
3. N. N. Garif'yanov, V. Yu. Maramzin, G. G. Khaliullin and I. A. Garifullin, *J. Exp. Theor. Phys.*, 1995, **80**, 301.
4. C. S. Guo, S. Yin and T. Sato, *Nanosci. Nanotechnol. Lett.*, 2011, **3**, 413.
5. C. S. Guo, S. Yin, L. Huang and T. Sato, *ACS Appl. Mater. Interfaces*, 2011, **3**, 2794.
6. C. S. Guo, S. Yin, Q. Dong and T. Sato, *Cryst. Eng. Comm.*, 2012, **14**, 7727.
7. C. S. Guo, S. Yin, M. Yan and T. Sato, *J. Mater. Chem.*, 2011, **21**, 5099.
8. C. Guo, S. Yin, Q. Dong and T. Sato, *Nanoscale*, 2012, **4**, 3394.
9. K. Adachi and M. Miratsu, *J. Mater. Res.*, 2010, **25**, 510.
10. H. Takeda, H. Kuno and K. Adachi, *J. Am. Ceram. Soc.*, 2008, **91**, 2897.
11. K. L. Purvis, G. Lu, J. Schwartz and S. L. Bernasek, *J. Am. Chem. Soc.*, 2000, **122**, 1808.
12. K. Adachia, *J. Mater. Res.*, 2012, **27**, 965.
13. Y. Sato, M. Terauchi and K. Adachi, *J. Appl. Phycol.*, 2012, **112**, 074308.
14. K. Adachi, Y. Ota, H. Tanaka, M. Okada, N. Oshimura and A. Tofuku, *J. Appl. Phys.*, 2013, **114**, 194304.
15. H. Takeda and K. Adachi, *J. Am. Ceram. Soc.*, 2007, **90**, 4059.
16. M. R. Skokan, W. G. Moulton and R. C. Morris, *Phys. Rev. B*, 1979, **20**, 3670.
17. C. S. Guo, S. Yin, M. Yan, M. Kobayashi, M. Kakihana, and T. Sato, *Inorg. Chem.*, 2012, **51**, 4763.
18. C. Guo, S. Yin, Y. F. Huang, Q. Dong and T. Sato, *Langmuir*, 2011, **27**, 12172.

The table of contents entry: Mo-containing $(NH_4)_xWO_3$ was synthesized by a solvothermal process and exhibited low infrared transmittance with an actual Mo/W (mol.) of 0.159.